

# Correlation of Single-Board Computer Ground-Test Data and On-Orbit Upset Rates from the Gaia Mission

D.L. Hansen, E. Ecale, R. Hillman, F. Meraz, J. Montoya, P. Paulet, E. Serpell, P. Tatry, G. Williamson

**Abstract**— Data Device Corporation’s (DDC) SCS750 single board computers (SBC) have been operating without interruption on board the Gaia satellite since its launch in 2014. The uninterrupted operation is possible because of several hardening techniques that allow the SBC to correct single event upsets (SEU) in the constituent components. We present on-orbit SEU data for the SBCs. All errors analyzed here were corrected by the SBC and had no effect on mission operation. We analyze the data to determine the accuracy of current models, as well as the effects of the space weather environment.

**Index Terms**— SEU, single event upset, heavy ion, heavy-ion testing, radiation, single event effects, solar particle events, space.

## I. INTRODUCTION

WITH the goal of cataloging nearly a billion stars to create the largest, most precise map of the Milky-Way Galaxy, the European Space Agency’s Gaia mission - for which Airbus Defense and Space, (Toulouse, France) is the prime contractor - provides an example of the capabilities enabled by high-performance computing. Gaia has been operating in a sun-centric orbit at the L2 point since January 2014, and uses seven identical video processing units (VPUs) to command the CCDs in the focal plane. Each VPU runs identical software with parameter settings that may differ [1]. Gaia produces about 50 Gbytes of data each day for downlink following onboard data processing and compression.

In this paper, we present on-orbit, upset-data from the CPUs and SDRAM in the DDC SCS750 single board computers (SBC) used in the Gaia VPUs. Both the CPUs and SDRAM are commercial parts for which a variety of hardening techniques work together to ensure fault-free performance of the SCS750. By providing access to a number of technologies not available in rad-hard foundries, the use of commercial, off-

the-shelf (COTS) technologies enables high-performance computing in satellites[2]-[3]. However, the harsh radiation environment in space provides a significant obstacle to the use commercial parts, and care must be taken in the system architecture to address environmental stresses.

The data presented here represents a success story. The DDC SCS750 uses rad-hard parts in conjunction with radiation mitigated COTS parts. In all cases, the errors reported here had no effect on mission. All were detected and corrected within the SCS750. The triple redundant processing architecture, which uses triple-mode redundancy (TMR), resynchronization, and scrubbing, was successful in enabling the spacecraft to operate through several periods of severe space weather with no ill effects to the system.

## II. GROUND TEST RESULTS

### A. Power PC

At the heart of the SCS750 are three PowerPC (PPC) CPUs operated with TMR. Detection hardware compares the output of each processor and disables any upset processor until it can be resynchronized by the scrubbing routine. This method protects the entire device including the processors, caches and registers [4].

Details of the SEE testing of the PPCs used in the SCS750 are given elsewhere [4]-[5]. The Weibull parameters are summarized in Table I. To describe it briefly here, testing was performed at the Texas A&M Cyclotron Institute Radiation Effects Facility. Three different tests were performed. The first was a static register test where the processor was programmed with a one-word instruction in an infinite loop. After irradiation, the state changes were counted. In the second, application tests were performed dynamically, while running a Dhrystone benchmark. The results were compared to other, non-irradiated processors running the same program to determine the number of errors. In the dynamic test, the bits used were not always susceptible to upset, and as a result the measured cross section was lower.

In the third test, all 3 processors on the SCS750 were irradiated simultaneously to test the effectiveness of the TMR mitigation scheme. Testing results were consistent with the calculated results [6]-[7] of the TMR configuration using data from the individually irradiated devices.

Manuscript received March 1, 2018.

D.L. Hansen, R. Hillman, F. Meraz, J. Montoya, and G. Williamson are with Data Devices Corp., San Diego, CA 92123 USA. e-mail:hansen@ddc-web.com.

P. Paulet, E. Ecale, P. Tatry are with Airbus Defence and Space SAS, Toulouse, France

E. Serpell is with the European Space Agency

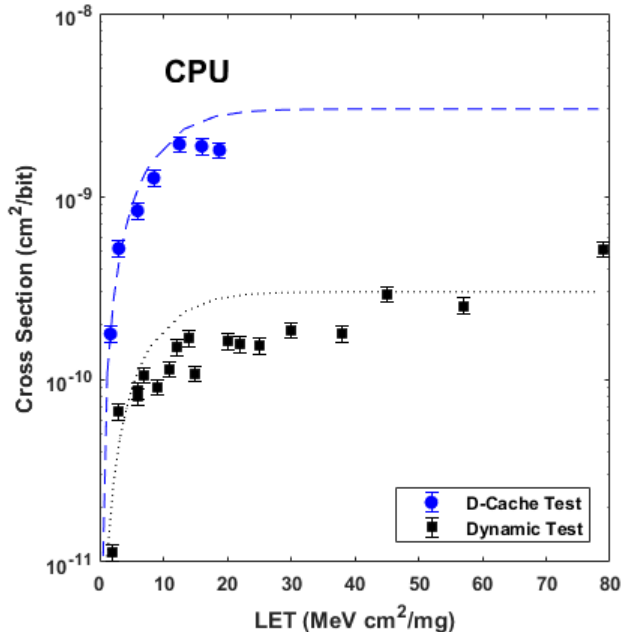


Fig. 1 CPU cross section data

TABLE I  
WEIBULL PARAMETERS FOR PPC AND SDRAM SEU

Device	$L_0$ (MeV cm <sup>2</sup> /mg)	W	s	$\sigma_{SAT}$ (cm <sup>2</sup> /bit)
PPC	0.1	10	1.5	$3.0 \times 10^{-9}$
SDRAM	0.95	50	2.8	$2.7 \times 10^{-9}$

### B. SDRAM

The SDRAM's in the SCS750 use advanced Reed-Solomon configured as 64 data bits, and 32 check bits. This detects and corrects any two-device failures, giving board level SEE immunity to these memory devices [4]. Reed-Solomon is a symbol-type correction-method and we record single- and double-nibble errors. No double nibble errors were detected so we assume all single-nibble errors represent single bad bits.

For the SDRAM (Fig. 2) data was collected at Texas A&M using parts programmed in the “inverse bleed down” pattern. In the SDRAM, the “bleed-down” pattern is the state toward which the data will relax if not refreshed. This was determined by periodically reading the memory without refreshing the data. In general, the tendency is for an entire row to bleed down to all “0’s” or all “F’s”. The inverse of the bleed-down pattern was determined to be the worst-case data pattern for SEU testing, with the device showing a higher cross-section for 1 to 0 upsets.

The SDRAM was tested in static and dynamic mode. For static mode, the part was initialized and the pattern verified. The device was irradiated with auto refreshes, and memory errors were counted following irradiation. In the dynamic test, the entire memory was written and verified using two words per row. During irradiation the following modes were tested: auto refresh idle, auto refresh power down, write/read with the inverse bleed down pattern, and write/read with the bleed down pattern.

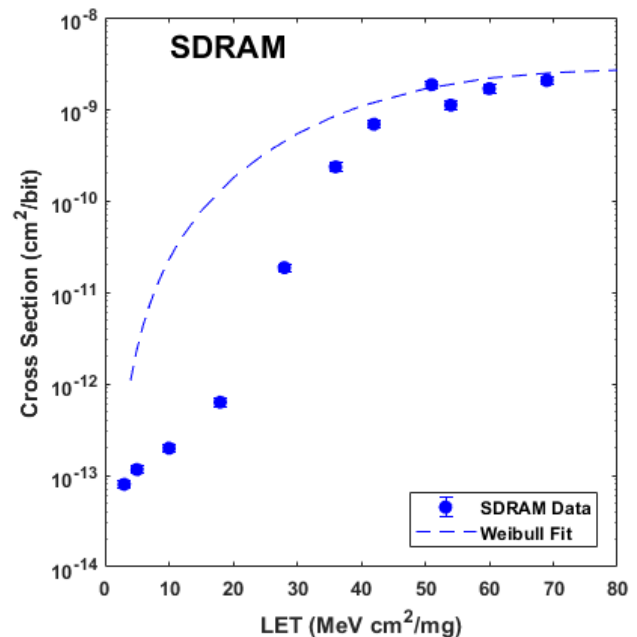


Fig. 2 SEU Cross Section and Weibull fit for the SDRAM

SEUs were distinguished from SEFI's by looking at the number of errors per word. More than two errors in a word accompanied by multiple rows where the majority of the words had an error, were considered to be caused by a SEFI. All other errors were considered SEUs. In the case of the SDRAM, we fit the data with a Weibull from the literature [8]. While the saturated cross section was similar for both data sets, the Weibull proves to be conservative, overestimating the low LET data points (Fig. 2).

### III. ON-ORBIT PERFORMANCE

While GAIA is operating in an L2 orbit, we model the environment using a geosynchronous (GEO) orbit assuming 100 mils (Al) shielding. This was done because assuming a GEO orbit makes it possible to use CREME96 [9]-[10] for the calculations and the environment expected in L2 and GEO is similar, with no trapped protons.

TABLE II  
CALCULATED UPSET RATES FOR PPC AND SDRAM SEU

Device	CREME96	CREME09 (Nymmik)
	GSM (UBD)	GSM (UBD)
PPC	$6.6 \times 10^{-8}$	$6.5 \times 10^{-8}$
SDRAM	$3.4 \times 10^{-11}$	$3.5 \times 10^{-11}$

For the CREME96 modeling, we selected the charge collection depth of 2  $\mu\text{m}$  with a funnel of 0.5  $\mu\text{m}$ . For the PPC, this provides an upper bound since partially depleted silicon-on-insulator (SOI) processes use tub depth between 0.15 and 0.18  $\mu\text{m}$  [5], [11]. The CREME suite of tools also includes a 2009 update (Nymmik) to the cosmic ray flux. Our results are similar to previously published data [12] that indicate GEO, solar-min, rates calculated with the CREME96 and Nymmik environmental models differ by less than 10% (Table II).

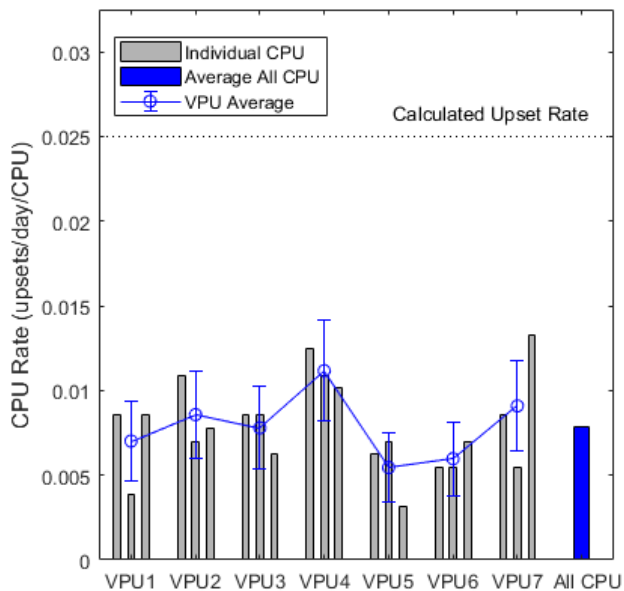


Fig. 3 Comparison of measured and calculated CPU upset rates. The three bars for each VPU label represent the three, TMR PPCs used in each SCS750. Error bars are calculated as the square root of the number of counts.

For the CPUs, we plot three different quantities in Fig. 3. First, the error rate for each CPU is plotted as a single bar with the three CPUs in the TMR configuration grouped by VPU. These bars represent the errors in a single processor corrected by the TMR architecture. Second, the final bar in the plot is the upset rate for all 12 CPUs. Finally, the error-bar plot gives the mean error-rate for the three CPUs within specific VPU with the error bars calculated as the square root of the number of upsets recorded.

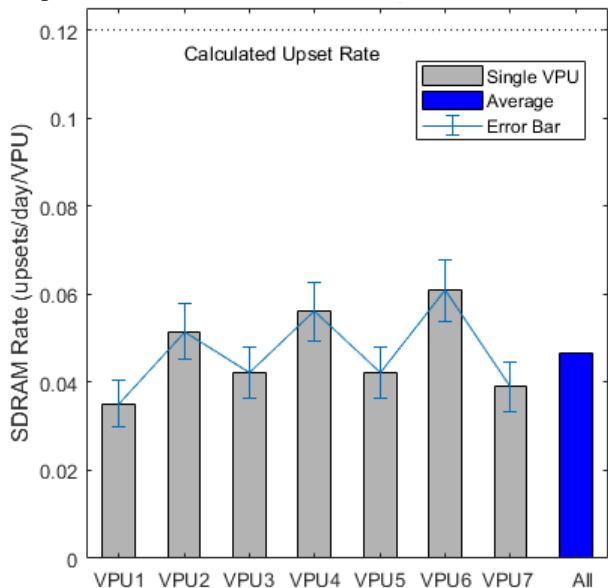


Fig. 4 Comparison of measured and calculated SDRAM upset rates. The bars labeled “VPU” represent the upset rate for the SDRAM in a single SCS750. Error bars are calculated as the square root of the number of counts.

The SDRAM data (Fig. 4) is displayed similarly. The “all” bar on the far right represents the average over all 7 VPUs, and the error bars are calculated in the same manner. However, the

VPU bars represent the average-SEU rate for all 12 die within a single VPU. No multi-nibble upsets were recorded.

For both the CPUs and the SDRAM, our results were similar to those found in [13] in that the calculated rate was about double the measured, on-orbit rate.

#### IV. DISCUSSION

In Fig. 5 we compare the upset rates with the proton flux for protons  $>10$  MeV measured by the GOES satellite. Since the upsets to the satellites typically come in at a low rate, the upset rate in these plots is the running average over 3 days.

NOAA Space Weather Prediction Center maintains a record of solar proton events [14]. Events during this data set are listed in Table III, and designated as the vertical dotted lines in Fig. 5. In Table III, we show the multiplication factors for the solar events and the SBC components. In cases where multiple events occurred in rapid succession, the multiplication factor was calculated over an interval including all events. The data in Fig. 5 indicates that the periods of highest proton flux seldom correspond to the periods of highest upset rate.

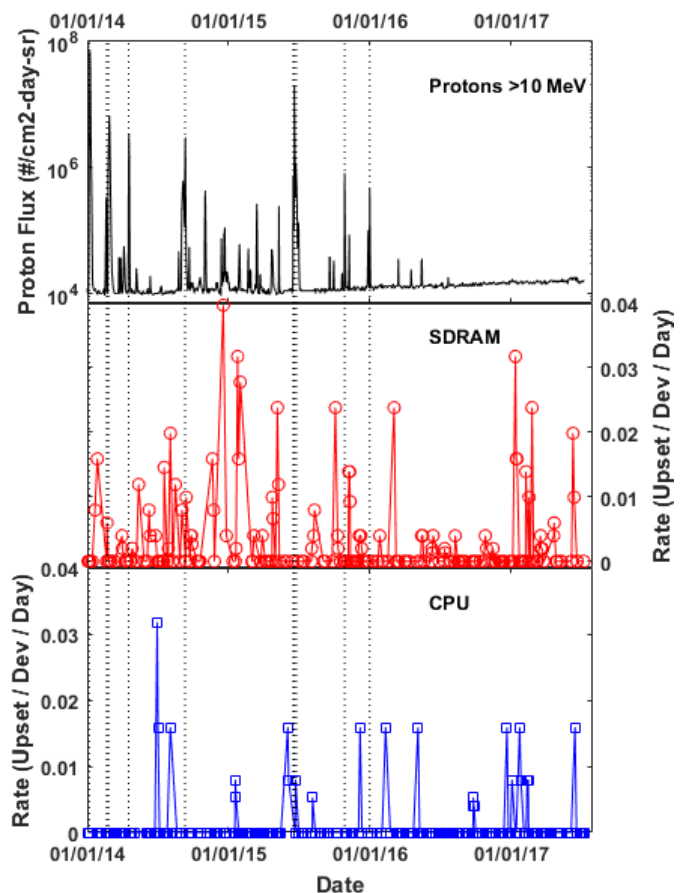


Fig. 5 Comparison of proton flux from GOES and on-orbit upset rates. Vertical lines represent the dates listed in Table III. NOAA solar-proton events are designated by the vertical dotted lines.

For comparison, we can also look at the galactic cosmic-ray (GCR) fluxes over this period using the data from the Cosmic Ray Isotope Spectrometer (CRIS) instrument on board the

Advanced Composition Explorer (ACE) satellite [15]. CRIS measures ionic composition and energy of galactic cosmic rays. The CRIS instrument detects 24 elements in 7 energy bands. Of the GCR elements present, carbon, oxygen, silicon, and iron are the most abundant of the more ionizing elements [16], and so for simplicity we will focus on these elements. In Table IV we tabulate the range of the energy bands as well as the corresponding LETs calculated using CREME-MC [17].

In Fig. 6, we plot the sunspot number and the GCR flux for C, Si, and Fe ions. The data follows the well-known pattern of GGR maximum coinciding with solar minimum. The most recent solar maximum period, which coincides with the data shown here, is associated with a smaller sunspot number and higher GCR flux than was seen in recent solar cycles. (Fig. 6).

TABLE III  
MULTIPLICATION FACTORS FOR SELECTED SOLAR PROTON EVENTS

Date[14]	10 MeV Proton	PPC	SDRAM
1/6/2014	6900	6.3	2.8
2/20/2014	688	2.8	4.3
2/25/2014			
4/18/2014	333	8	2.7
9/11/2014	290	2.3	2.6
6/18/2015			
6/21/2015	1900	1	1
6/26/2015			
10/29/2015	72	1	2.7
1/2/2016	41	1	1.5

TABLE IV  
ENERGY AND LET FOR SELECTED GCR SPECIES DETECTED BY CRIS

Ion	Z	Energy Range (MeV/n)	LET Range (MeV cm <sup>2</sup> /mg)
C	6	59.0 – 200.4	0.54 – 0.21
O	8	69.4 – 237.9	0.84 – 0.33
Si	14	94.8 – 322.6	2.0 – 0.82
Fe	26	129.1 – 471.0	6.0 – 2.4

In Fig. 7-8 we plot the GCR flux as a function of upset rate for the SDRAM and CPU. In general the increased flux correlates to a higher upset rate. However to look at the relationship quantitatively, we calculate the correlation coefficients ( $r$ ) for the upset rates and ion fluxes (Tables V-VI) for 10-day and 100 day averages of the data ( $r_{10}$  and  $r_{100}$  respectively). Discussion of calculating  $r$  can be found elsewhere [18] in general the coefficient takes on the values  $-1 \leq r \leq 1$  with values closer to 0 indicating the variables are less likely to be linearly correlated. For the 100 days averages, over the duration of the data we would have a total of  $N=12$  periods over which the data was averaged, while for the 10 day averages we have  $N=120$  periods.

To better understand the significance of the coefficients, we first discuss the probability of uncorrelated variables producing the correlation coefficients given in Table V. For the CPU upset rate and GCR flux, the probability that uncorrelated data would produce  $r_{100}=0.7$  is 1.1%, while the probability uncorrelated data would produce  $r_{10}=0.3$  is 0.2%. In contrast the correlation coefficient for protons and the CPU upset rate is no better than  $r_{10}=0.12$  which corresponds to 70% probability of uncorrelated variables.

In the case of the SDRAM (Table VI),  $r_{100}=0.3$  corresponds to a 34% probability of uncorrelated data, while  $r_{10}=0.1$  corresponds to a 32% chance that the flux is not correlated with the upset rate. We also note that for the SDRAM correlation to  $>10$  MeV protons  $r_{100}=-0.22$  (Table VI). This leads to the nonsensical conclusion that the increased proton flux actually decreases the SDRAM upset rate. However, the probability of an uncorrelated group of samples producing this result is about 53% and the result can be discarded on both statistical and intuitive grounds.

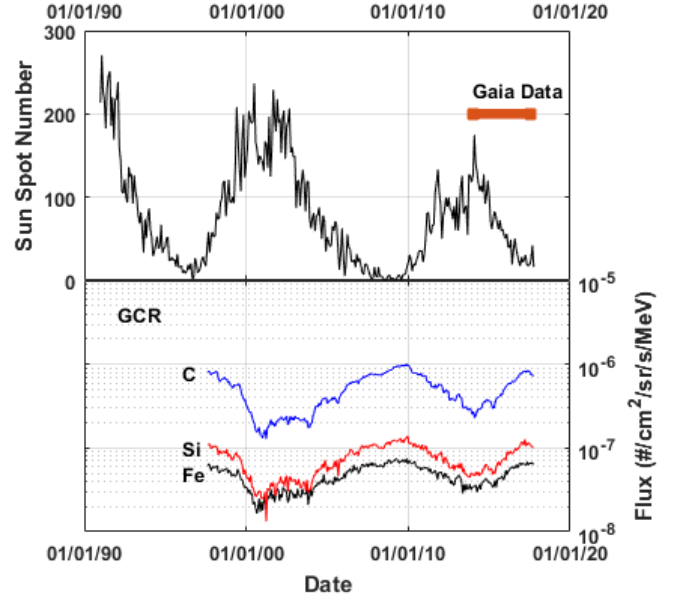


Fig. 6 Sun spot number [19] and Fe GCR flux from ACE-CRIS [15] for the past two solar cycles. On this scale, the C and O flux are nearly identical. Period of Gaia data is indicated by the bar in the top plot.

There are a number of trends evident from the correlation coefficients in Tables V-VI. First, the upset rates are correlated to the GCR ion fluxes, but not the solar proton fluxes. This may merely be a reflection of the fact that neither the SDRAM nor the CPU is a “good” proton detector. In the case of the SDRAM this may be partially accounted for by the high LET threshold of the cross section (Fig. 2). While we would expect the CPU to be sensitive to proton upsets based on the fact that the threshold is lower than 15 MeV cm<sup>2</sup>/mg, the upset rate for the PPC is low (Fig. 5) making it more difficult to measure the correlation. We also note that proton fluxes are measured by the GOES satellite in a GEO orbit, while Gaia is located at L2. However explaining the lack of correlation by differences in the space environment is in contrast to the conventional wisdom of using GEO environmental parameters to describe interstellar space [20].

Second, the CPU upset rate is more strongly correlated to the GCR fluxes than the SDRAM upset rate. This results from the difference in SEU sensitivity. The maximum LET of the ions plotted in the CRIS data (Table IV) is only 6 MeV cm<sup>2</sup>/mg. Over this LET range, the CPUs (Fig. 1) have a higher upset cross-section than the SDRAMs (Fig. 2), and are thus

more sensitive to changes in the fluxes measured by CRIS.

Finally, correlation between the upset rates and the GCR fluxes is much stronger when the data is averaged over a longer period (100 days vs 10 days). This corresponds to the fact that the GCR flux is increasing gradually over several years, and the devices studied upset at a relatively low rate. By averaging over the longer time period the significance of the stochastic variation in the device upset rate is reduced.

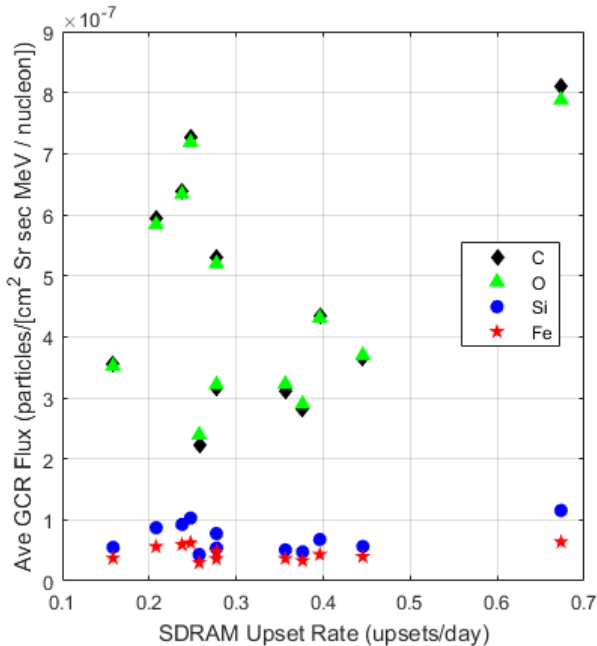


Fig. 7 Average of GCR flux vs. SDRAM upset rate for C, O, Si, and Fe. All values are 100 day averages

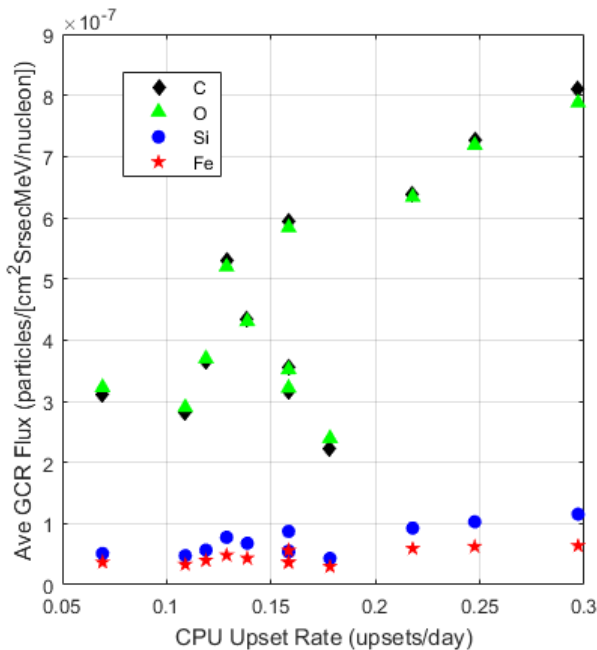


Fig. 8 Average of GCR flux vs. CPU upset rate for C, O, Si, and Fe. All values are 100 day averages.

TABLE V  
CORRELATION COEFFICIENTS FOR ION FLUX AND UPSET RATES FOR THE CPU

	100 Day Average	10 Day Average
--	-----------------	----------------

	$r_{100}$	Uncorrelated Probability	$r_{10}$	Uncorrelated Probability
Proton > 10 MeV	0.02	100%	0.12	32%
Proton > 100 MeV	0.11	77%	0.11	32%
C	0.77	1%	0.32	0.2%
O	0.77	1%	0.32	0.2%
Si	0.79	0.2%	0.34	<0.2%
Fe	0.73	1%	0.29	0.2%

TABLE VI  
CORRELATION COEFFICIENTS FOR ION FLUX AND UPSET RATES FOR THE SDRAM

	100 Day Average		10 Day Average	
	$r_{100}$	Uncorrelated Probability	$r_{10}$	Uncorrelated Probability
Proton > 10 MeV	-0.22	53%	-0.04	62%
Proton > 100 MeV	-0.01	100%	-0.002	100%
C	0.28	34%	0.12	32%
O	0.27	34%	0.1	32%
Si	0.29	34%	0.12	32%
Fe	0.20	53%	0.09	32%

## V. CONCLUSION

The SCS750 on board the Gaia mission has operated without interruption during periods of severe space weather. All errors recorded were corrected, allowing the mission to continue operation. Upset data for the Power PCs and SDRAMs collected during the transition from a weak solar-maximum to solar minimum is reported here. The data shows a much stronger correlation the GCR flux than to the solar proton flux.

## REFERENCES

- [1] Gaia Data Release 1, European Space agency and Gaia Data Processing and Analysis Consortium, on the web at: [https://gaia.esac.esa.int/documentation/GDR1/pdf/GaiaDR1\\_documentation\\_1.1.pdf](https://gaia.esac.esa.int/documentation/GDR1/pdf/GaiaDR1_documentation_1.1.pdf)
- [2] D. L. Hansen, K. Jobe, J. Whittington, M. Shoga and D. A. Sunderland, "Correlation of Prediction to On-Orbit SEU Performance for a Commercial 0.25- $\mu$ m CMOS SRAM," in IEEE Transactions on Nuclear Science, vol. 54, no. 6, pp. 2525-2533, Dec. 2007.
- [3] B. Peters, A. Wardrop, D. Lahti, H. Herzog, T. O'Connor and R. DeCoursey, "Flight SEU Performance of the Single Board Computer (SBC) Utilizing Hardware Voted Commercial PowerPC Processors On-board the CALIPSO Satellite," 2007 IEEE Radiation Effects Data Workshop, Honolulu, HI, 2007, pp. 16-25
- [4] R. Hillman, G. Swift, P. Layton, M. Conrad, C. Thibodeau and F. Irom, "Space processor radiation mitigation and validation techniques for an 1,800 MIPS processor board," Proceedings of the 7th European Conference on Radiation and Its Effects on Components and Systems, 2003. RADECS 2003, Noordwijk, The Netherlands, 2003, pp. 347-352.
- [5] F. Irom, F. F. Farmanesh, A. H. Johnston, G. M. Swift and D. G. Millward, "Single-event upset in commercial silicon-on-insulator PowerPC microprocessors," in IEEE Transactions on Nuclear Science, vol. 49, no. 6, pp. 3148-3155, Dec 2002.
- [6] L.D. Edmonds, "Analysis of Single-Event Upset Rates in Triple-Modular Redundancy Devices," JPL Publication 09-6, 2009.
- [7] G. Allen, L.D. Edmonds, G. Swift, C. Carmichael, C. Wei Tseng; K. Heldt, S.A. Anderson, M. Coe, "Single Event Test Methodologies and System Error Rate Analysis for Triple Modular Redundant Field Programmable Gate Arrays," *IEEE Trans. Nucl. Sci.*, Vol.58, pp.1040-1046, June 2011.
- [8] R. Koga, P. Yu, K. Crawford, S. Crain and V. Tran, "Comparison of heavy ion and proton-induced single event effects (SEE) sensitivities," in IEEE Transactions on Nuclear Science, vol. 49, no. 6, pp. 3135-3141, Dec 2002.
- [9] On the web at [https://ngdc.noaa.gov/stp/space-weather/interplanetary-data/solar-proton-events/SEP\\_page\\_code.html](https://ngdc.noaa.gov/stp/space-weather/interplanetary-data/solar-proton-events/SEP_page_code.html)

- [10] A. J. Tylka et al., "CREME96: A Revision of the Cosmic Ray Effects on Micro-Electronics Code," in *IEEE Transactions on Nuclear Science*, vol. 44, no. 6, pp. 2150-2160, Dec 1997.
- [11] S. K. H. Fung et al., "Controlling floating body effects for 0.13  $\mu\text{m}$  and 0.10  $\mu\text{m}$  SOI CMOS," in 2000 IEDM Technical Digest, pp. 231–234.
- [12] A. L. Bogorad, J. J. Likar, R. E. Lombardi, S. E. Stone and R. Herschitz, "On-Orbit Error Rates of RHBD SRAMs: Comparison of Calculation Techniques and Space Environmental Models With Observed Performance," in *IEEE Transactions on Nuclear Science*, vol. 58, no. 6, pp. 2804-2806, Dec. 2011.
- [13] J. J. Likar, A. L. Bogorad, R. E. Lombardi, S. E. Stone and R. Herschitz, "On-Orbit SEU Rates of UC1864 PWM: Comparison of Ground Based Rate Calculations and Observed Performance," in *IEEE Transactions on Nuclear Science*, vol. 59, no. 6, pp. 3148-3153, Dec. 2012.
- [14] List of CME dates is found on the web at [https://ngdc.noaa.gov/stp/space-weather/interplanetary-data/solar-proton-events/SEP\\_page\\_code.html](https://ngdc.noaa.gov/stp/space-weather/interplanetary-data/solar-proton-events/SEP_page_code.html)
- [15] <http://www.srl.caltech.edu/ACE/ASC/datadocs.html>
- [16] P. M. O'Neill, "Badhwar–O'Neill 2010 Galactic Cosmic Ray Flux Model—Revised," *IEEE Trans. Nucl. Sci.*, vol. 57, no. 6, pp. 3148-3153, Dec. 2010.
- [17] On the web at <https://creme.isde.vanderbilt.edu/>
- [18] J.R. Taylor, *An Introduction to Error Analysis*, Mill Valley, CA: University Science Books, 1982, p. 180.
- [19] <http://www.swpc.noaa.gov/products/solar-cycle-progression>
- [20] The CREME96 tool uses the same environment for "Near-Earth Interplanetary," and "Geosynchronous Orbit" in the FLUX module.